RSC Advances

This article can be cited before page numbers have been issued, to do this please use: M. V. Parmekar and A. V. Salker, *RSC Adv.*, 2016, DOI: 10.1039/C6RA21942J.

ROYAL SOCIETY OF CHEMISTRY

www.rsc.org/advances

View Article Online
DOI: 10.1039/C6RA21942J

Journal Name

ARTICLE

Room temperature complete reduction of nitroarenes over novel $Cu/SiO_2@NiFe_2O_4$ nano-catalyst in aqueous medium – A kinetic and mechanistic study

Received 00th January 20xx,
Accepted 00th January 20xx

DOI: 10.1039/x0xx00000x

www.rsc.org/

Mira V. Parmekar and A. V. Salker*

The current investigation reports preparation of a novel system $Cu/SiO_2@NiFe_2O_4$ as characterised by XRD, XPS, IR, SEM-EDS, TEM, ICP-AES and VSM data. Its catalytic activity was explored in nitroarene reduction using 4-Nitrophenol as the model substrate for studying reaction kinetics. The studies revealed the rate constant of the reaction at RT to be 0.325 min^{-1}. Each test reaction here contained only 10.6 µg of copper wherein the activity factor was 0.511 sec^{-1} mg^{-1} which is by far the highest for any non-noble metal catalyst reported for this reaction. Also the energy of activation of the reaction was found to be 30.4 K J mol^{-1} which falls in the lower range of average E_{act} reported in literature for the reaction under study. Further insights on the reaction pathway indicated the reaction followed the direct route for nitro reduction via formation of a nitroso derivative. Overall we present here an economical, efficient and environmentally benign methodology for nitroarene reduction using the designed catalyst.

1. Introduction

Metal and metal oxide nanoparticles have taken the centre stage in heterogeneous catalysis ever since their discovery.[1–5] The major reason for this is the high surface area it provides for a reaction, along with faster reaction rates and better selectivity as compared to its bulk counterparts. The only area where not much has changed is its separation; either it has to be done by filtration or ultracentrifuge. Considering the fine nature of the nanoparticles even with much effort, it is very difficult to remove all the catalyst materials by these techniques. For the same reason even after so much progress has been made in nano-catalysis, industrialisation of the procedures is still in the backseat. The newer wave of nano-catalysts somehow has come with a solution for the same viz. magnetisation.[6,7]

Nitrophenol and its derivatives are significant by-products produced from industries producing pesticides, herbicides and synthetic dyes.[8] These industries thus result in large amount of wastewater with a high content of residual pollutants even after the conventional post-treatment methods, most of which is released to the environment. To effectively deal with wastewater containing aromatic pollutants, many approaches have been explored including membrane separation, occulation–coagulation, adsorption, oxidation or ozonation, photocatalytic degradation, chemical reduction with the catalyst assistance, and aerobic or anaerobic treatment.[9]

Department of Chemistry, Goa University, Taleigao-Goa, India, 403206.
Email: sal_arun@rediffmail.com; sav@unigoa.ac.in
Electronic Supplementary Information (ESI) available: See DOI: 10.1039/x0xx00000x

Catalytic reduction of harmful nitro compounds has received much attention lately due to such rising pollution issues as well as the industrial importance of its beneficial amino counterparts.[9] For example; 4-Nitrophenol (4-NP) is a recognised industrial pollutant listed on "Priority Pollutant List" by U.S. Environmental Protection Agency attributing to its toxicity, potential carcinogenicity, as well as mutagenicity.[8,10] The product 4-aminophenol (4-AP) in turn finds use in preparation of some tuberculostatic, antipyretic and analgesic drugs, as photographic developer, anti-corrosion additive in paints and so on.[11] Although many methods have been cited in literature to deal with the stated problem but catalytic reduction to the amino derivative still remains the most efficient and economic practice till date.[12] At a time like this turning to heterogeneous catalyst for solution isn't a surprise owing to their high efficiency, clean processing, easy operation, and low cost. However, most catalysts reported for reduction reaction are noble metal based resulting in higher production cost thus hindering their practical application.[9] This leaves a void in the research field to be filled up by alternative efficient, cheaper and preferably greener methodologies.

In our attempt to do so we designed a novel Cu based catalyst material for the nitro-reduction of aromatics. The developed nano-catalytic system has Cu supported on silica coated nickel ferrite; shortened as $Cu/SiO_2@NiFe_2O_4$. Being magnetic, the catalyst provides added advantage of being completely separable using an external magnet, while silica coating increases stability of the magnetic particles in solution by preventing agglomeration.[13–15] The kinetics of the reaction revealed that it behaves as an excellent catalyst for complete reduction of 4-NP to 4-AP with stoichiometric excess of $NaBH_4$

View Article Online
DOI: 10.1039/C6RA21942J

at ambient conditions in water, the cheapest and greenest solvent available. Also a series of nitroarenes were reduced in presence of the designed catalyst giving complete conversion with excellent yields. Fortunately enough we could also trace the presence of nitroso derivative formed as an intermediate during the course of reduction and thus decisively propose a detailed mechanistic pathway of how the reaction occurs.

2. Experimental

2.1 Materials

For all experimental procedures doubly distilled water was used. All chemicals used for catalyst syntheses were obtained from Sigma Aldrich and used as it is. $NaBH_4$ used was of AR grade obtained from Thomas Baker. The nitroarenes were of commercially available reagent grade.

2.2. Methods

The prepared catalyst samples were characterised by IR spectroscopy recorded on Shimadzu IR prestige 21 spectrophotometer and XRD pattern recorded on a Rigaku diffractometer, using Cu Kα radiation (λ = 1.5418 Å, filtered through Ni filter) to obtain its structure and phase. The XPS analysis was carried out to determine surface composition with PHI5000 Versa Probe II model. The morphology of catalysts was determined using Zeiss Avo18 Scanning Electron Microscope (SEM). Particulate size confirmation were done by Transmission Electron Microscopy (TEM) recorded on Philips CM 200 electron microscope (resolution = 2.4 Å). Energy dispersive X-ray spectroscopy (EDS) was recorded on an Oxford instrument. Cu percentage was determined using Inductive Coupled Plasma Atomic Emission Spectroscopy (ICP-AES) with SPECTRO Analytical Instruments ARCOS Simultaneous ICP Spectrometer model. All the kinetic reactions were monitored using Agilent tech UV-Vis Spectrophotometer. GC analysis were carried out on 5765 Nucon equipment fitted with OV101 column. VSM data was recorded with Quantum design Versa Lab instrument.

2.3. Preparation of $Cu/SiO_2@NiFe_2O_4$

A slight modified citrate gel combustion technique was utilised for the preparation of nickel ferrite support material.[16,17] In brief, calculated amounts of the metal nitrates with 1:2 metal to citrate ratio was taken in aqueous medium. The combined solution was stirred on a hotplate for around an hour for homogenisation. Following this it was subjected to heat till most of the water evaporated resulting in a viscous gel. This was then introduced in a uniform heating oven for combustion. The combusted gel was calcined at 400 °C for 4 h and later at 600 °C for 2 h to remove any residual carbon.

For silica coating on the nickel ferrite Stöber process was employed.[18,19] Herein at first the magnetic ferrite was dispersed in ethanol-water mixture (2: 1 ratio) and sonicated for homogeneity. A calculated volume of liquor ammonia was added to this mixture followed by drop wise addition of TEOS under vigorous stirring. The solution thus obtained was subjected to 6 h moderate stirring at RT. The $SiO_2@NiFe_2O_4$ so formed was then separated by an external magnet, washed with distilled water and ethanol and dried at 70 °C.

Cu deposition on the support was achieved by wet impregnation method which was further reduced using $NaBH_4$. Briefly in a 100 mL beaker 500 mg $SiO_2@NiFe_2O_4$ was dispersed in 30 mL distilled water. To this required amount of $Cu(NO_3)_2$ was added and kept for vigorous stirring. After about 20 minutes $NaBH_4$ solution was introduced in the beaker in parts reducing copper to its metallic state. The whole mixture was kept stirring for 2 - 3 h for uniform distribution of the metal on the support. The black powder so obtained was then magnetically separated, washed with copious amount of distilled water and finally ethanol. It was dried at 80 °C overnight before use. A graphical representation for the whole protocol is shown below.

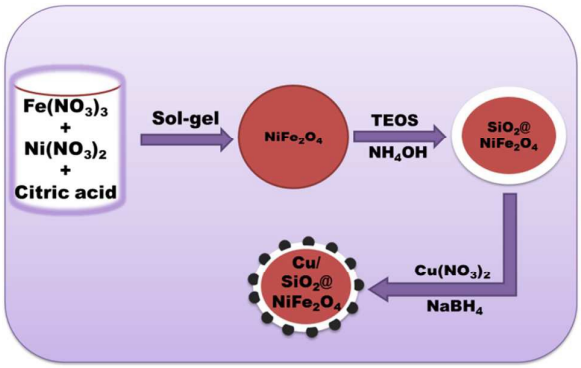

Scheme 1. Pictorial depiction of preparation of $Cu/SiO_2@NiFe_2O_4$.

2.4. Experimental procedure for kinetic study of catalytic reduction of 4-Nitrophenol

The kinetic studies pertaining to catalytic reduction were carried out in quartz cuvettes with 1 cm path length using a total aqueous volume of 2.9 mL. For each test, a known volume of the catalyst suspension ranging from 50-100 µL was taken from 800 ppm catalyst stock, 100 ppm w.r.t. Cu (0.8 mg in 1 mL water) in the cuvette and dispersed in distilled water to make up a total volume of 1 mL. To this was added 1 mL of 2.16×10^{-4} M aqueous 4-NP solution. Just before placing in the UV-Vis instrument 0.9 mL of freshly prepared aqueous 0.04 M NaBH4 was introduced in the cuvette which resulted in an increased colour intensity of the reaction mixture to an intense yellow-green colour (Bathochromic shift). Immediately the absorption spectra were recorded on UV-Vis spectrophotometer at room temperature in the range of 200 - 600 nm.

2.5. General procedure for nitroarene reduction over catalyst

0.2 mmol of the nitroarene was dissolved in 5 mL 1:1 MeOH - H_2O mixture. To this was added 2.5 mg of the catalyst and stirred for a while. Immediately 2 mmol of $NaBH_4$ was added to this in parts and stirred till end of the reaction. The reaction was monitored throughout by TLC/GC using aliquots removed at regular time intervals. The removed aliquots were extracted using ethyl acetate in miniature glass tubes. At the end of the reaction, the catalyst was separated from the

View Article Online
DOI: 10.1039/C6RA21942J

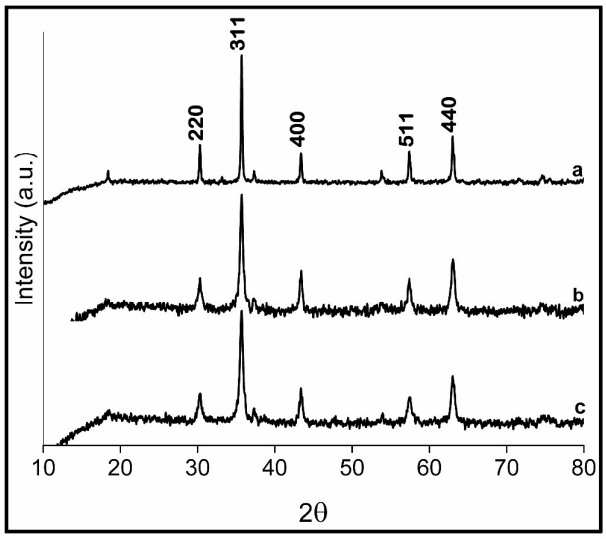

Fig. 1. XRD pattern of synthesised samples a) $NiFe_2O_4$, b)SiO_2@$NiFe_2O_4$, and c)Cu/SiO_2@$NiFe_2O_4$.

reaction mixture using an external magnet, rinsed with water followed by acetone and dried at 80 ºC for reuse.

3 Results and discussion

3.1. Catalyst Characterisation

3.1.1 Structure determination

The XRD pattern (Fig. 1a) is an exact match to cubic nickel ferrite (JCPDS card 003-0875) with 2θ = 35.72 as the 100% intensity peak. SiO_2 coated nickel ferrite sample does not show much difference in the pattern obtained and so does the Cu supported sample (1c). This is suggestive of the fact that both SiO_2 and Cu are uniformly distributed over the magnetic ferrite resulting in no extra peaks.[14] Its presence was further confirmed by means of IR, EDS and TEM data. The broadening

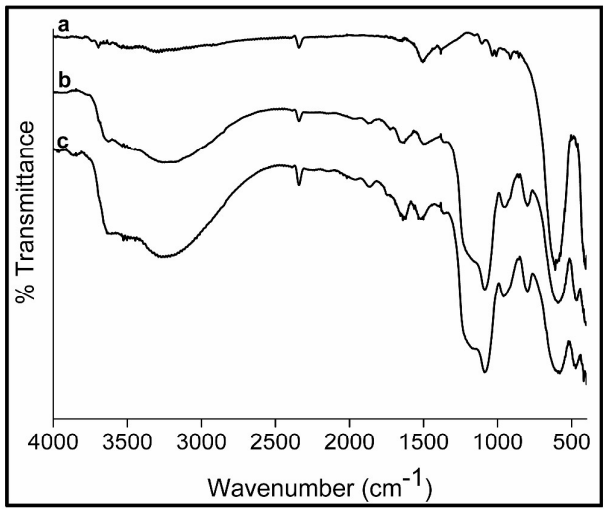

Fig. 2. IR spectra of synthesised samples a) $NiFe_2O_4$, b) SiO_2@$NiFe_2O_4$, and c)Cu/SiO_2@$NiFe_2O_4$.

of the XRD peaks could be arising due to amorphous silica coating.[13] The IR data too supports the information as a broad band in the region 1000-1200 cm^{-1} is seen (Fig. 2b, c) which is the characteristic frequency of Si-O-Si stretching. Also distinct Fe-O stretching around 590 cm^{-1} is observed in all the IR spectra.

3.1.2. Size and shape of the catalyst

As the prepared catalytic system had to be tested for heterogeneous reaction, it was of significance to determine its surface characteristics. Keeping this in mind we carried out imaging analysis of the samples using scanning electron microscopy (SEM) and transmission electron microscopy (TEM). The images obtained can be seen in Fig. 3. On closer observation of the TEM images it is visible that the ferrite particles are quasi-spherical in nature. Fig. 3e shows clearly a uniform coat of silica covering the magnetic core. Also SEM and TEM images of Cu supported sample shows the presence of fine particles over the silica coat (3f). The average particle sizes as obtained from TEM images were 25 - 28 nm for the synthesised samples which were higher than the crystallite sizes calculated by Scherrer equation D = Kλ/βCosθ from the XRD data. Electron diffraction (ED) pattern shown as insets in Fig. 3 confirms highly crystalline nature of samples. Inset in Fig. 3e evidently specifies the increased degree of amorphosity due to silica coating which is elevated further in Cu/SiO_2@$NiFe_2O_4$ (3f inset). Also from the obtained ED patterns, d values were calculated which matched the ones in the XRD spectrum and thus was indexed to the cubic phase (Fig.S1).

Along with SEM, EDS and ICP-AES were also carried out to know the percentage composition of the active species in the sample. Results clearly indicated presence of Cu in 12.69% and 13.22% in the active sample by EDS and ICP-AES respectively. The elemental mapping data clearly showed uniform distribution of Si as well Cu on the ferrite support further confirming their presence as well (ESI).

The XPS data was recorded to investigate the oxidation state of surface Cu deposited on silica coated nickel ferrite. Fig. 4a displays a survey scan of all the elements present in the active sample. The high resolution Cu 2p region scan (Fig. 4b) reflects two clear peaks with 19.8 eV difference in B.E. values at 931.2 eV and 951 eV respectively for Cu 2p3/2 and 2p1/2 indicating it to be present majorly in the reduced state.[20,21] It can't be convincingly stated though whether Cu is present in majority as Cu^+/Cu^0 on the silica surface as the B.E. for both are very close. The presence of not so prominent satellite peaks in the region 940 eV indicates it to be slightly oxidised to CuO. Overall we conclude that surface Cu is present in mixed oxidation states major being the reduced state. The remaining individual elemental spectrum can be seen in ESI.

The Fe 2p spectrum (Fig. S2) shows presence of 2 peaks at B.E. 711.5 eV and the satellite peak 8.2 eV higher which is characteristic of Fe in +3 oxidation state.[22,23] The high resolution spectrum of Ni 2p (Fig. S2) shows presence of satellite peak on the higher side of B.E. scale indicating Ni to be in +2 oxidation state. On de-convolution Ni 2p3/2 peak

View Article Online
DOI: 10.1039/C6RA21942J

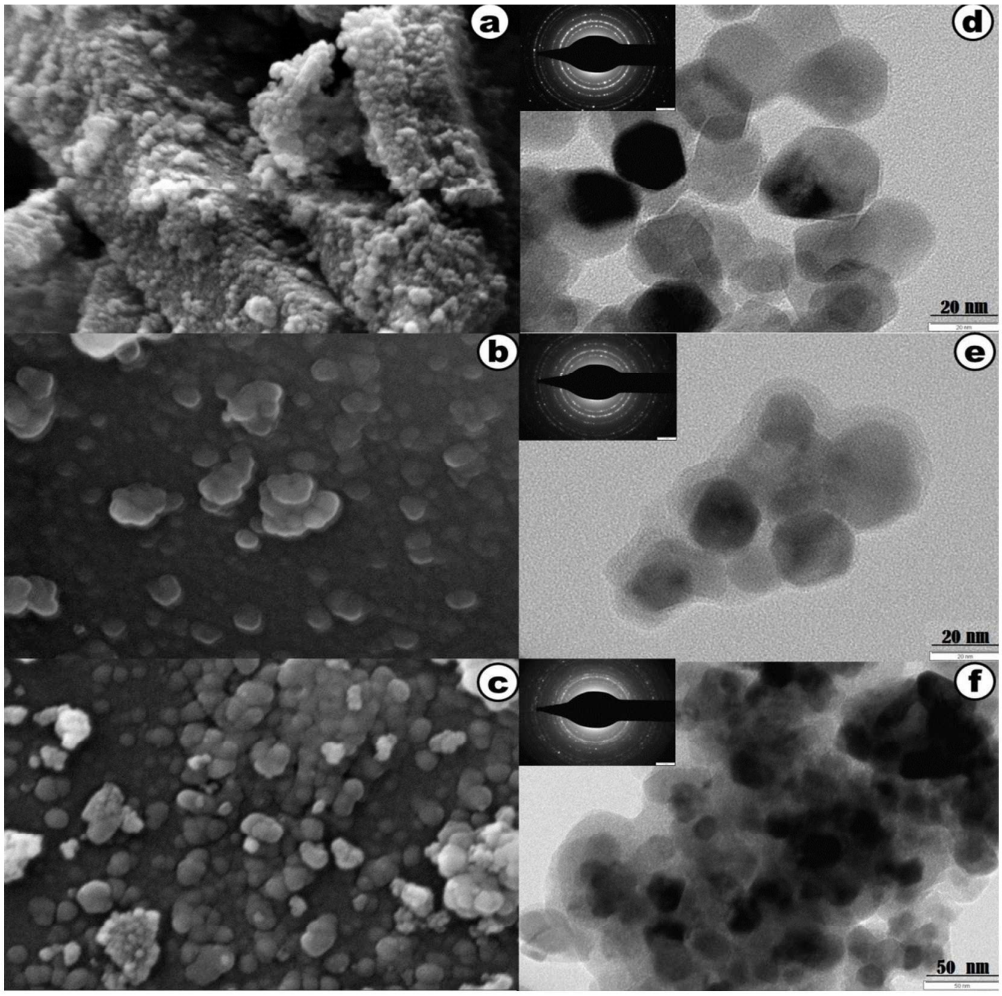

Fig. 3. SEM and TEM images of $NiFe_2O_4$ (a, d), SiO_2@$NiFe_2O_4$ (b, e) and Cu/SiO_2@$NiFe_2O_4$ (c, f).The inset in fig d, e, f represents the ED pattern for the respective sample.

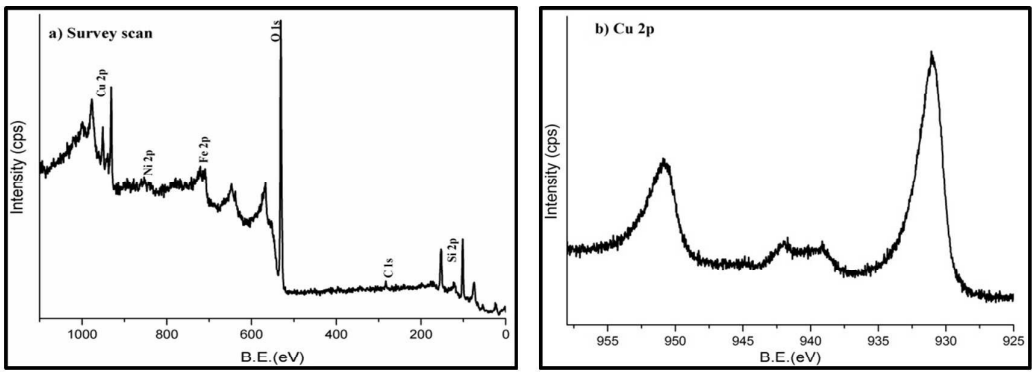

Fig. 4. XPS spectra of Cu/SiO_2@$NiFe_2O_4$ showing (a) survey scan and (b) Cu 2p region.

resolved into a doublet with B.E. 854.6 and 856 eV confirming the presence of non-equivalent tetrahedral and octahedral sites.[23] At last the 1s region scan for O in Fig. S2. shows one peak at 531.2 eV with a shoulder at 528.3 eV pointing to the fact the catalyst sample is a metal oxide. Thus we can certainly say that the intended system Cu/SiO_2@$NiFe_2O_4$ is formed.

3.1.3. Magnetic property

The synthesised system was prepared with the intention of easy separation by an external magnet as has a magnetic core

View Article Online
DOI: 10.1039/C6RA21942J

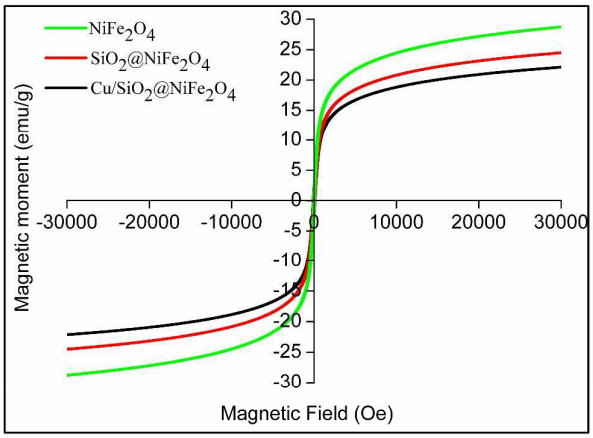

Fig. 5. Room temperature magnetisation curves of the synthesised samples.

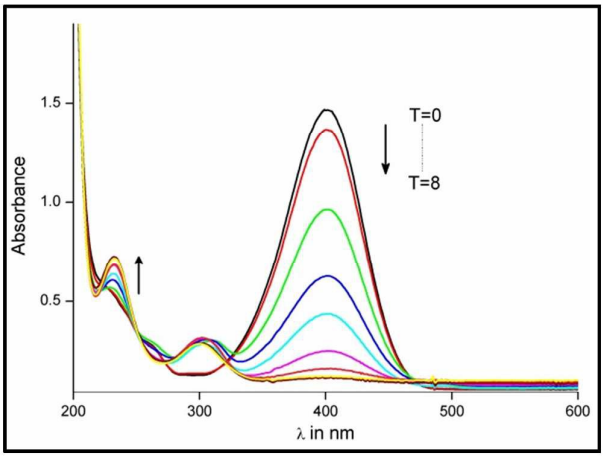

Fig. 6. UV-Vis contour displaying course of 4-NP reduction showing every 1 min change.

and therefore was subjected to room temperature VSM analysis for studying its magnetic properties. The applied magnetic field was increased from zero to a maximum of 3T. As expected the saturation magnetisation (Ms) was highest for $NiFe_2O_4$ which decreased after silica coating and was found lowest for $Cu/SiO_2@NiFe_2O_4$ as seen in the Fig. 5. Opposite trend is seen for coercivity though (Table S1). A Ms value of 22.12 emu g^{-1} for the sample of interest was indicative of the fact that it is magnetic.

3.2. Catalytic activity studies over the catalyst

The catalytic activity of the sample was tested for room temperature nitro reduction reaction using 4-NP as the model substrate. Various control experiments were carried out to find the efficiency of the catalyst as shown in Table 1. It is quite visible from the obtained results that of all the synthesised samples, $Cu/SiO_2@NiFe_2O_4$ system showed the best catalytic activity under the given reaction conditions.

Table 1
Different Catalysts tried for 4-NP reduction using 0.9 mL of 0.04 M $NaBH_4$.

Entry	Catalyst	Conversion in 7min (%)[b]	K (min^{-1})
1	No Catalyst	-[c]	-
2	Fe_3O_4	traces	0.005
3	$NiFe_2O_4$	8	0.013
4	$SiO_2@NiFe_2O_4$	traces	0.002
5	$50\%Cu/Fe_3O_4$	80	0.170
6	$Cu/SiO_2@NiFe_2O_4$	100	0.325

[a] Reaction conditions: 4-NP (1 mL, 2.16 x 10^{-4} M), catalyst (80 mg), RT.
[b] Monitored by UV-Vis
[c] No conversion was seen even after 5 days.
*Note: Cu/SiO_2 works fine for the reaction but due to the fine nature of silica could not be separated after reaction as it was not magnetically separable.

The time dependant studies for 4-NP reduction reaction were performed using UV-Vis spectrophotometer with pre-programmed kinetics method wherein it was possible to record in-situ progress of the reaction. As soon as 4-NP solution came in contact with $NaBH_4$ a bathochromic shift is observed in its absorption frequency (λ_{max}) from 317 nm to 400 nm.[24]

This is a result of formation of phenolate ion of the substrate in alkaline conditions. As the reaction progressed the absorption at λ_{max}= 400 nm decreased over time and two new λ_{max} appeared at 226 nm and 300 nm which is characteristic of 4-AP. A complete conversion of 4-NP to 4-AP was obtained within 7 minutes in presence of 10.58 µg Cu (3.48 ppm Cu) in a total volume of 2.9 mL. Also, the UV-Vis contour (Fig. 6) confirms the formation of 4-AP as the sole product in the reaction which is further established by the NMR of isolated product (S3). Each of the test samples employed only 0.9 mL of 0.04 M $NaBH_4$ which is very less as compared to what have been reported in literature. Although it is quiet in excess as compared to the concentration of 4-NP (1 mL, 2.16 x 10^{-4} M), so the reaction eventually proceeds via pseudo first order kinetics.

3.2.1 Kinetics of 4-NP reduction

Following the pseudo first order kinetics law, the rate of the reaction can be directly co-related to the concentration of 4-NP, which in turn is relative to the absorbance of the medium at any given time t. Thus the ratio of the absorption at a given

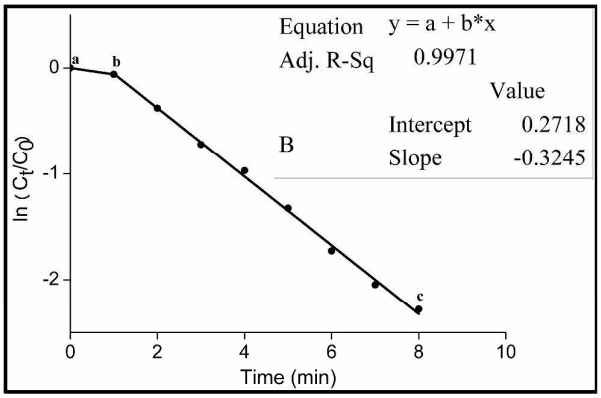

Fig.7. First order kinetics plot for obtaining *k* value of 4-NP reduction.

View Article Online
DOI: 10.1039/C6RA21942J

time is directly proportional to the ratio of the concentration of 4-NP, i.e. $A_t/A_0 = C_t/C_0$ (as per Beer-Lambert's law).
To calculate the rate constant we simply plot ln (C_t/C_0) ^{v}/s time as seen in Fig. 7 which depicts an exponential decay curve. Slope of the steepest part of the curve (bc) gives the rate constant *k* for the reaction. For all the experimental tests the portion marked 'ab' in Fig. 7 indicated delay in the start of the reaction or the so called induction time. It is described as the time required for the substrate molecules to properly align and get adsorbed on to the catalyst surface. The same phenomenon has been earlier reported by other researchers as well.[8,25]

Table 2
Rate constant values obtained with varying amounts of catalyst.

Entry	Catalyst loading (µg)	Cu content (µg)	*k* (min^{-1})
1	80	10.58	0.139
2	72	9.52	0.164
3	64	8.46	0.207
4	56	7.40	0.237
5	48	6.35	0.255
6	40	5.29	0.325

3.2.2. Effect of catalyst amount

Table 2 summarises the data obtained with different amounts of catalyst per test keeping all the other reaction parameters constant. Initially the reaction was started with 5.29 µg Cu loading and increased up to 10.58 µg in the medium. It is very much evident from the table that the value of rate constant *k* is dependent on the amount of catalyst used and increases proportionately with increase in Cu amount. Interestingly, *k* value of 0.325 min^{-1} (5.42 x 10^{-3} sec^{-1}) was obtained with mere 5.29 µg Cu (3.48 ppm Cu) at RT. To compare with the ones reported in literature we calculated the activity factor (K) given as the ratio of *k* over milligram of active catalyst used in the reaction.[26,27] Surprisingly K for our system was found to be 0.511 sec^{-1} mg^{-1} which is higher than any previous reports in literature for Cu or any non-noble metal catalyst. Also on comparison it was realised that K in the present investigation is lesser only to Pt/thin film, Pd/magnetite-KCC-1 and Au/CeO_2 NTs, all of which are tedious to prepare as well as contain noble metals which are very expensive as compared to Cu if industrialisation of the protocol is considered.[10,28,29] Just for an overview we have tabulated comparison of a few recent examples with our designed catalyst in Table 3.

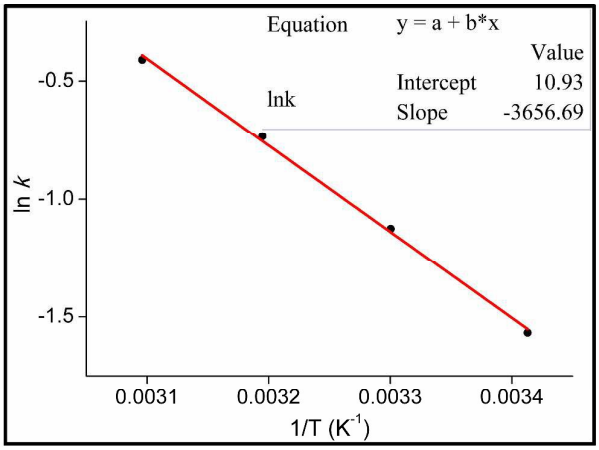

Fig. 8. Plot of ln *k* v/s 1/T for calculating E_{act} of the reaction.

3.2.3 Effect of temperature

The temperature gradient studies were carried out in the range 20-50 ºC. The obtained results are plotted in Fig. S4 which goes well with Arrhenius theory. As expected it was discovered that *k* increases with increase in temperature. Even at a low concentration of 3.48 ppm Cu the reaction rate went as high as 0.663 min^{-1} at 50 ºC. The average activation energy (E_{act}) for 4-NP reduction is ~44 KJ mol^{-1}.[8] A plot of ln *k* v/s 1/T was plotted to calculate the same for the reaction (Fig. 8) using the designed catalyst and was found to be 30.4 KJ mol^{-1}. This is one of the lowest values of E_{act} reported for this reaction.[25,30,31]

3.3 Recyclability

A key aspect in designing a magnetically separable catalyst is

Table 3
Comparison of Activity factors K* reported in literature for various catalysts.

Entry	Catalyst	Active species (mg)	*k* in sec^{-1}	Activity factor K (sec^{-1}. mg^{-1})	Ref.
1	$CuO/\gamma\text{-}Al_2O_3$	0.5000	0.0050	0.010	35
2	H40-PEI-PEG-stabilised AuNPs	0.1960	0.0033	0.017	36
3	Fe_3O_4 @SiO_2/EP.EN.EG@Cu	0.0584	0.0032	0.055	14
4	Cu porous microspheres	0.0600	0.0043	0.072	37
5	Cu 9.5 nm Cubes	0.0960	0.0101	0.105	31
6	Pd/SPB-PS	0.0380	0.0044	0.116	38
7	Au/grapheme hydrogel	0.0240	0.0031	0.129	26
8	Cu -1 nanoplate	0.0700	0.0095	0.136	27
9	AgNPs/SNTs-4	0.2700	0.0384	0.142	39
10	Fe_3O_4@SiO_2@Dendritic-SiO_2-NH_2-Ag	0.0300	0.0145	0.483	19
11	Ni–Pt nanoparticles (96 : 4)	0.0040	0.0019	0.485	40
12	**Cu/SiO_2@$NiFe_2O_4$**	**0.0106**	**0.0054**	**0.511**	**This work**

* The values are either obtained or calculated from the data given in the respective articles.

View Article Online
DOI: 10.1039/C6RA21942J

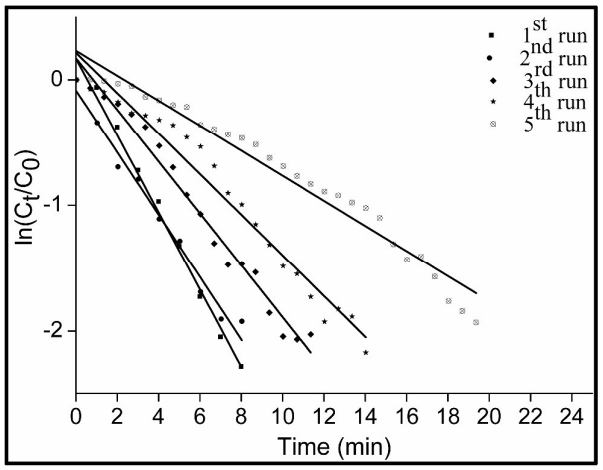

Fig.9. Recyclability plot for reduction of 4-NP.

to test its recycling ability. Here again progress of the reaction was monitored using UV-Vis spectrophotometer as usual. This was carried out for 5 cycles and the results tabulated in Table S2. It is evident from Fig. 9 that the catalyst showed 100% conversion for each test run but the time span per cycle increased relatively. The reason for this we predict could be loss of catalyst during separation after each test run or due to blocking of active sites by the product molecules. The product 4-AP, an amine is well known in literature for poisoning catalyst when present even in minute quantities.[32,33] This results in unavailability of active sites on the catalyst for reacting species to react leading to slower reactivity. Also a noteworthy observation was that there was no induction period for the subsequent recycle runs as compared to the fresh catalyst run. This further confirms the probability that there were not many active sites available after the subsequent test runs for the reacting substrate to engage with the catalyst resulting in no delay time and consequently decreased reactivity. Although considering the fact that each test run employed only 10.58 µg Cu still could be efficient for 5 consecutive run cycles in less than 1 h is quite remarkable.

3.4. Leaching test

For supported catalysts leaching studies designate the benchmark of its efficiency and reusability. Considering this we performed the said tests following a simple protocol. The reduction reaction was carried out typically in a quartz cuvette ensuring the standard reaction conditions. After 4 minutes, the entire reaction medium was transferred in an identical cuvette except the catalyst which was retained using an external magnet. The UV-Vis spectra of the medium in the second cuvette were continually recorded for 100 minutes. There was no appreciable change in the absorbance once the catalyst was removed. Even on keeping the solution standing for a week, the yellow colour persisted. This is an indication that no appreciable loss of active Cu from the catalyst surface takes place during the reaction. To confirm this further, we scaled up the reaction to 2 mmol scale and recovered the catalyst after 1st and 5th cycle. The recovered catalyst was then subjected to

Table 4
Nitroaromatic derivatives studied for nitroreduction reaction[a] using the catalyst.

General reaction showing conversion of nitro to amino functionality

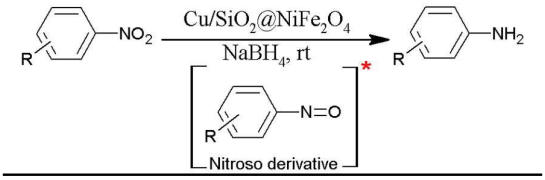

Entry	Substrate	Time (min)	Conversion[b] (%)	Yield[c] (%)
1	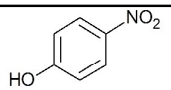	12	100	100[d]
2	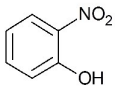	20	>99	>99
3	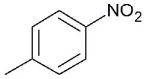	20	100	>99
4	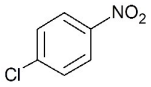	40	100	100
5	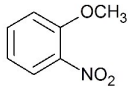	40	100	100
6	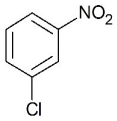	60	100	83
7	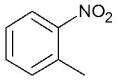	80	100	100
8	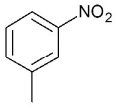	80	100	95
9	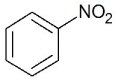	90	100	>95
10	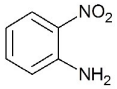	100	100	100
11	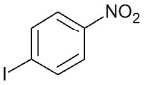	210	60	59

[a] Reaction conditions: Nitroarene (0.2 mmol), $NaBH_4$ (2 mmol) and catalyst (2.5 mg) in 1:1 H_2O-MeOH (5 mL).

[b] % Conversion was calculated by GC using n-decane as the internal standard. For comparison of R_t values of the reactants as well as expected products authentic reference samples were used.

[c]
$$\%\ \text{Yield of the product} = \frac{\text{Area of product of interest}}{\text{Area of all products}} * 100$$

[d] Isolated yield, reaction was carried out on 1mmol scale.

View Article Online
DOI: 10.1039/C6RA21942J

ICP-AES analysis. The results obtained showed negligible loss of Cu (0.03%) after the first run although after 5th run the total loss of Cu was 0.5%. This also could be one of the reasons for decrease in activity over the catalyst in recyclability studies. Thus it can be conveniently stated that no appreciable loss of Cu was observed in the reaction conditions employed and the pathway followed for the reaction was heterogeneous one.

3.5. Variable nitroarene reduction studies

To know the scope of catalytic activity of $Cu/SiO_2@NiFe_2O_4$ in nitro reduction reaction, reduction of various nitroarenes were tried in presence of the synthesised catalyst. Solvent studies inferred 1: 1 MeOH - H_2O to be the best solvent for the reaction as most of the substrates being organic molecules showed low solubility in water alone (Table S3).

Excellent yields were obtained for all the derivatives as can be seen in Table 4. Except for 1-Iodo-4-nitrobenzene all samples showed complete conversion within specified amount of time. Other functionalities like –OH, –Cl, $–CH_3$, $–NH_2$, remained unaltered during the reduction process. Thus it can be concluded that the developed methodology could be used as an economical, efficient and environmentally benign nitro reduction technique.

3.5.1. Reaction Mechanism

rearrangement of catalyst surface to best accommodate the reactant molecules. In other words it indicates adsorption of the 4-NP molecules on the catalyst surface by a reversible process. This phenomenon is precisely described by Ballauff et al. stating how the kinetics of 4-NP reduction over SPB is governed by the above mechanism.[25] They also mentioned reversible adsorption of boro-hydride on metal catalyst being one of the fast reactions in the cascade of steps. Both the above adsorption steps take place simultaneously on the catalyst surface. Adsorbed 4-NP is then reduced by the surface hydrogen moieties which is the rate determining step. 4-AP formed, then detaches from the catalyst surface leaving it free to react all over again. As per the LH mechanism desorption reactions are also assumed to be fast steps. A pictorial representation of the same is given in the graphical abstract.

3.5.2. Mechanistic Pathway

As mentioned in literature the two established mechanistic pathways for nitro reduction are shown in scheme 2 viz; Direct and Condensation route [13,24]. As the intermediate for Nitrobenzene reduction are commercially available we carried out mechanistic studies using this substrate. Authentic samples of the intermediates, nitrosobenzene (direct route) and azobenzene (condensation route) were first injected onto the GC and its retention time (R_t) was noted. Subsequently,

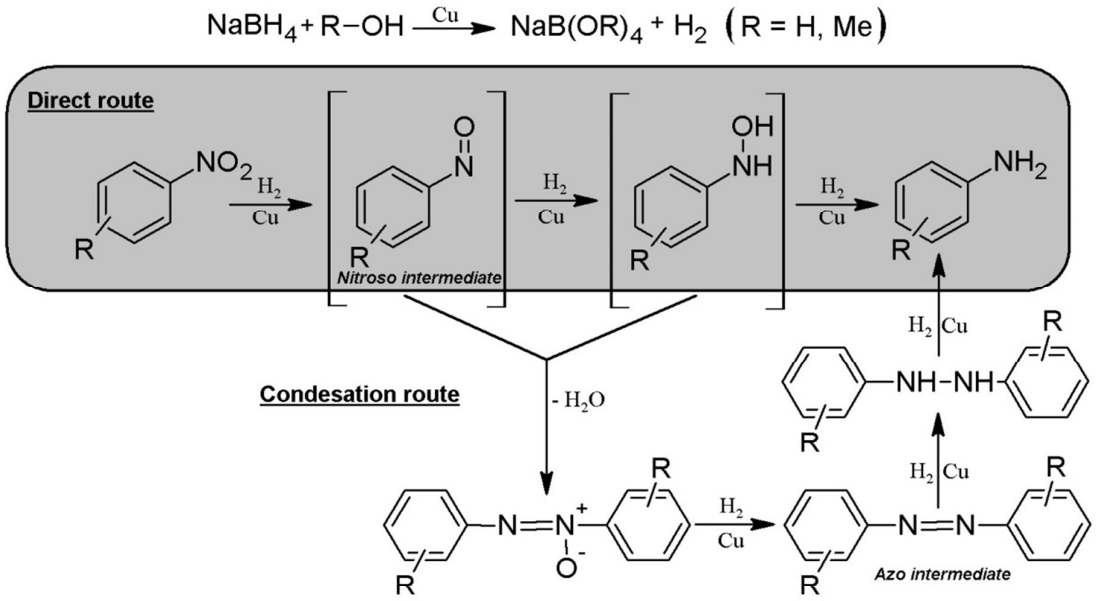

Scheme 2: Mechanistic pathway for nitro reduction over $Cu/SiO_2@NiFe_2O_4$.

The literature reports propose various mechanisms for nitro reduction over metal nanoparticles.[8] Of these the closest match to all the inferences for the Cu catalyst system is the Langmuir-Hinshelwood mechanism (LH). LH mechanism advocates reaction occurring due to the interaction between molecular fragments and atoms adsorbed over the catalyst surface.[34] As mentioned earlier we observed a delay in the start of the reaction which was presumed due to the nitrobenzene (0.2 mmol) was subjected to reduction under the same conditions as mentioned above with aliquots being analysed every 15 minutes on GC until the reaction was complete (analysis details and reaction progress studies are given in SI). The aliquot at 15 min showed presence of 4 peaks besides the solvent peak. Of these one was of nitrobenzene, one of aniline, one matched nitrosobenzene R_t and the extra peak we presumed to be of phenyl hydroxylamine which

View Article Online
DOI: 10.1039/C6RA21942J

disappeared in the subsequent aliquots. Thus we can say then conversion of phenyl hydroxylamine to aniline is a kinetically favourable step and occurs relatively fast. Surprisingly the reaction aliquot showed no peak at reference R_t of azobenzene matching the authentic sample.

For further verification the same reaction was carried out on both the intermediates, viz; nitrosobenzene and azobenzene separately. It was realised that within half an hour nitrosobenzene showed 100% conversion and gave aniline as the sole product, while azobenzene remained at only 56% conversion at the end of four hours also selectively giving only aniline as the product. Thus we decisively say that the reaction of nitro reduction over our catalyst proceeded via direct route only as proposed in Scheme 2.

4. Conclusions

As per our observations, $Cu/SiO_2@NiFe_2O_4$ shows much better activity for 4-NP reduction as compared to other samples tested. This indicated that the activity is solely due to finely dispersed Cu on the magnetic support. Considering the percentage of Cu present in the total amount of catalyst used per test it is quite remarkable that such low quantity of catalyst could give such high activity. It also could be successfully recycled for 5 consecutive run cycles within 1 h. As per the kinetic studies we obtained a very high rate constant of 0.325 min^{-1} with just 10.58 µg Cu (3.48 ppm Cu) in the catalyst which is noteworthy.

Even the obtained E_{act} for the system of 30.4 K J mol^{-1} is remarkably low. To the best of our knowledge the obtained activity factor of 0.511 sec^{-1} mg^{-1} is by far the lowest for any non-noble metal catalyst for the said reaction. Given the fact that nitroso-benzene could be traced as being formed as the intermediate during the reduction of nitrobenzene, a well-established mechanistic pathway could be assigned with authorization for the course of the reduction process. Hence we hereby report non-noble and comparatively inexpensive $Cu/SiO_2@NiFe_2O_4$ as a novel catalytic system for 4-NP reduction with high *k*, low E_{act} and highest K reported till date, as well as a methodology which could very well be classified as green, highly efficient as well as an economical protocol for nitroarene reduction in general.

Acknowledgements

Authors thank UGC-BSR for financial assistance.

References

1 V. Polshettiwar and R. S. Varma, *Green Chem.*, 2010, **12**, 743–754.
2 D. Jagadeesan, *Appl. Catal. A Gen.*, 2016, **511**, 59–77.
3 S. Babu and B. R. Jagirdar, *ChemSusChem*, 2012, **5**, 65–75.
4 L. L. Chng, N. Erathodiyil and J. Y. Ying, *Acc. Chem. Res.*, 2013, **46**, 1825–1837.
5 R. Narayanan, *Green Chem. Lett. Rev.*, 2012, **5**, 707–725.
6 R. Hudson, Y. Feng, R. S. Varma and A. Moores, *Green Chem.*, 2014, **16**, 4493–4505.
7 M. B. Gawande, P. S. Branco and R. S. Varma, *Chem. Soc. Rev.*, 2013, **42**, 3371–3393.
8 T. Aditya and T. Pal, *Chem. Commun.*, 2015, **51**, 9410–9431.
9 H. Hu, J. H. Xin, H. Hu, X. Wang, D. Miao and Y. Liu, *J. Mater. Chem. A*, 2015, **3**, 11157–11182.
10 X. Le, Z. Dong, Y. Liu, Z. Jin, T. Huy, M. Le and J. Ma, *J. Mater. Chem. A Mater. energy Sustain.*, 2014, **2**, 19696–19706.
11 J. R. Chiou, B. H. Lai, K. C. Hsu and D. H. Chen, *J. Hazard. Mater.*, 2013, **248-249**, 394–400.
12 H. Lu, H. Yin, Y. Liu, T. Jiang and L. Yu, *Catal. Commun.*, 2008, **10**, 313–316.
13 R. K. Sharma, Y. Monga and A. Puri, *J. Mol. Catal. A Chem.*, 2014, **393**, 84–95.
14 M. Rajabzadeha, H. Eshghia, R. Khalifehb and M. Bakavolia, *RSC Adv.*, 2016, 19331–19340.
15 M. B. Gawande, Y. Monga, R. Zboril and R. K. Sharma, *Coord. Chem. Rev.*, 2015, **288**, 118–143.
16 K. Pradhan, S. Paul and A. R. Das, *Catal. Sci. Technol.*, 2014, **4**, 822–831.
17 K. Faungnawakij, R. Kikuchi, N. Shimoda, T. Fukunaga and K. Eguchi, *Angew. Chem. Int. Ed. Engl.*, 2008, **47**, 9314–9317.
18 K. Yu, X. Zhang, H. Tong, X. Yan and S. Liu, *Mater. Lett.*, 2013, **106**, 151–154.
19 Z. Sun, H. Li, G. Cui, Y. Tian and S. Yan, *Appl. Surf. Sci.*, 2016, **360**, 252–262.
20 S. M. D. Watson, N. G. Wright, B. R. Horrocks and A. Houlton, *Langmuir*, 2010, **26**, 2068–2075.
21 Z. Zheng, J. Yu, S. Cheng, Y. Lai, Q. Zheng and D. Pan, *J. Mater. Sci. Mater. Electron.*, 2016, **27**, 5810–5817.
22 R. Singh Yadav, J. Havlica, J. Masilko, L. Kalina, J. Wasserbauer, M. Hajdúchová, V. Enev, I. Kuřitka and Z. Kožáková, *J. Magn. Magn. Mater.*, 2015, **394**, 439–447.
23 A. B. Nawale, N. S. Kanhe, K. R. Patil, S. V. Bhoraskar, V. L. Mathe and a. K. Das, *J. Alloys Compd.*, 2011, **509**, 4404–4413.
24 A. A. Vernekar, S. Patil, C. Bhat and S. G. Tilve, *RSC Adv.*, 2013, **3**, 13243–13250.
25 S. Wunder, F. Polzer, Y. Lu, Y. Mei and M. Ballauff, *J. Phys. Chem. C*, 2010, **114**, 8814–8820.
26 J. Li, C. Liu and Y. Liu, *J. Mater. Chem.*, 2012, **22**, 8426–8430.
27 Y. Sun, L. Xu, Z. Yin and X. Song, *J. Mater. Chem. A*, 2013, **1**, 12361–12370.
28 S. J. Hoseini, M. Rashidib and M. Bahramia, *J. Mater. Chem.*, 2011, **21**, 16170–16176.
29 J. Zhang, G. Chen, M. Chaker, F. Rosei and D. Ma, *Appl. Catal. B Environ.*, 2013, **132-133**, 107–115.
30 X. Wu, X. Wu, J. Shen and H. Zhang, *RSC Adv.*, 2014, **4**, 49287–49294.
31 P. Zhang, Y. Sui, G. Xiao, Y. Wang, C. Wang, B. Liu, G. Zou and B. Zou, *J. Mater. Chem. A*, 2013, **1**, 1632–1638.
32 Y. Du, H. Chen, R. Chen and N. Xu, *Chem. Eng. J.*, 2006, **125**, 9–14.
33 A. Baiker, I. Monti and Y. S. Fan, *J. Catal.*, 1984, **88**, 81–88.
34 P. Atkins and J. De Paula, in *Atkin's Physical Chemistry*, Oxford University Press, 9 edition., 2010, p. 898.
35 S. U. Nandanwar and M. Chakraborty, *Chinese J. Catal.*, 2012, **33**, 1532–1541.

View Article Online
DOI: 10.1039/C6RA21942J

36 Y. Dai, P. Yu, X. Zhang and R. Zhuo, *J. Catal.*, 2016, **337**, 65–71.
37 S. Gao, X. Jia, J. Yang and X. Wei, *J. Mater. Chem.*, 2012, **22**, 21733–21739.
38 Y. Mei, Y. Lu, F. Polzer, M. Ballauff and M. Drechsler, *Chem. Mater.*, 2007, **19**, 1062–1069.
39 Z. Zhang, C. Shao, Y. Sun, J. Mu, M. Zhang, P. Zhang, Z. Guo, P. Liang, C. Wang and Y. Liu, *J. Mater. Chem.*, 2012, **22**, 1387–1395.
40 S. K. Ghosh, M. Mandal, S. Kundu, S. Nath and T. Pal, *Appl. Catal. A Gen.*, 2004, **268**, 61–66.

View Article Online
DOI: 10.1039/C6RA21942J

Graphical Abstract: Select one of the two

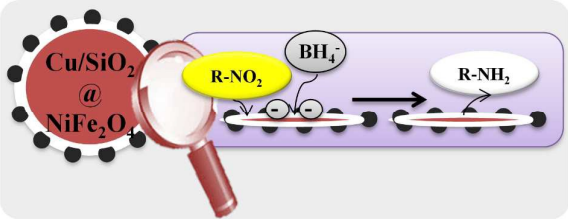

Schematic representation of surface reaction on the catalyst

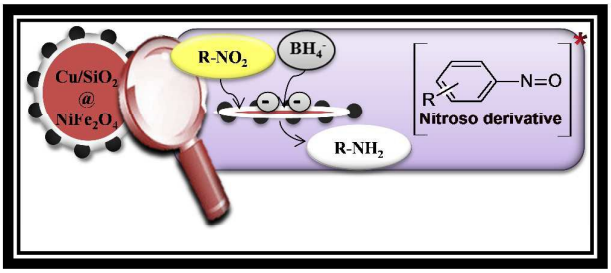

Schematic representation of surface reaction on the catalyst